International Journal of Refractory Metals and Hard Materials 118 (2024) 106435

Contents lists available at ScienceDirect

International Journal of Refractory Metals and Hard Materials

journal homepage: www.elsevier.com/locate/IJRMHM

Improved mechanical and tribological properties of TiAlN coatings by high current pulsed electron beam irradiation

Qingfeng Guan [a], Jing Han [a], Shiyu Zhou [b], Jintong Guan [a,*], Conglin Zhang [c], Fuyang Cao [a,*], Xiangming Chen [b]

[a] School of Materials Science and Engineering, Jiangsu University, Zhenjiang 212013, China
[b] Zhuzhou Cemented Carbide Cutting Tools Co., Ltd, Zhuzhou 412007, China
[c] School of Materials Science and Engineering, Yancheng Institute of Technology, Yancheng 224051, China

ARTICLE INFO

Keywords:
TiAlN coating
High current pulsed electron beam (HCPEB)
Hardness
Scratch adhesion
Wear resistance

ABSTRACT

High current pulsed electron beam (HCPEB) irradiation is an important surface engineering technique, which has been proved to be valid in modifying the surface microstructure and properties of various materials. In this work, HCPEB was employed to irradiate TiAlN coatings. The microstructure, mechanical and tribological properties of both original and irradiated TiAlN coatings were investigated. The results showed that the surface roughness of the TiAlN coatings first increased with 5 pulses of HCPEB irradiation, and then gradually declined with a further increase in pulse numbers. Compared with the original coating, the coating irradiated by 15 pulses demonstrated superior hardness (up to 33.4 GPa) and adhesion strength (112N), excellent wear resistance (wear rate of 3.3×10^{-6} mm^3/Nm) and low friction coefficient (0.37). It is believed that the grain refinement, formation of the transition zone and adjustment of residual stresses after 15 pulses of HCPEB treatment are responsible for the improvement in both mechanical and tribological properties of the TiAlN coatings. These findings might suggest the potential applications of HCPEB irradiation for surface modification and hardness improvement of hard nitride coatings.

1. Introduction

Hard coatings have been commonly used to protect tools and components by virtue of their high hardness, excellent wear resistance and thermal stability [1–3]. The ternary Ti-Al-N system, by incorporating Al into TiN, shows superior oxidation resistance and mechanical properties. Currently, TiAlN coatings are demonstrated to be one of the most widely used coatings for high-speed cutting and dry machining [4]. Ion plating is one of the most commonly adopted physical vapor deposition (PVD) techniques to prepare TiAlN coatings [5]. However, the inevitable side effects of this method are the defects such as macroparticles (so-called droplets), pores on the coating surface, and excessive residual stress in the as-deposited coating [6–8]. These drawbacks might lead to high surface roughness or coating delamination, etc., thus greatly limit the performance of TiAlN coatings. As such, great efforts have been made to improve the surface morphology, microstructure, residual stress and mechanical properties of the TiAlN coatings [9–13].

Recently, high current pulsed electron beam (HCPEB) processing of coatings has attracted increasing attention from both academia and industry. As an advanced surface treatment method, HCPEB can induce flash melting of the surface followed by a rapid solidification, resulting in significant changes in microstructure, and thus its corresponding mechanical and other aspects of properties [14–16]. For instance, Perry et al. [17] found that HCPEB irradiation resulted in an increased density of cracks in PVD TiN coatings, while removed atomic level defects, vacancies and dislocations, as well as residual stress. Weigel et al. [18] found that high-flux electron beam treatment had minor influence on the morphology and crystallinity of the $Ti_{1-x}Al_xN$ phase, however, the stress-free lattice parameter and compressive stress in the coatings were reduced.

To date, few investigations have been reported concerning HCPEB irradiation on PVD TiAlN coatings. And the effect of electron beam irradiation on the mechanical and tribological properties of TiAlN coatings remains unclear. In this work, the effect of HCPEB irradiation on the surface morphology, nano-hardness, scratch adhesion and wear performance of PVD TiAlN coatings was studied. The underlaying

* Corresponding author.
E-mail address: fuyangcao@ujs.edu.cn (F. Cao).

https://doi.org/10.1016/j.ijrmhm.2023.106435
Received 19 August 2023; Received in revised form 17 October 2023; Accepted 18 October 2023
Available online 21 October 2023

mechanisms were also clarified and discussed.

2. Experimental details

2.1. Coating preparation

TiAlN coatings with a thickness of 2–3 μm were deposited on YG6 cemented carbide substrates by arc ion plating system (Oerlikon Balzers INNOVA). The substrates in 12 × 12 × 4.8 mm were first grounded with sandpapers from 150 to 7000 grits, polished to a mirror surface, ultrasonically cleaned in acetone for 30 min, and then dried before placing in the vacuum chamber for clamping. The base pressure in the reaction chamber was better than 2×10^{-4} Pa. Before deposition, the substrates were cleaned by glow discharge in Ar (99.99%) for 30 min with a substrate bias of −500 V, and the substrate temperature was set to be 500 °C. The deposition process of TiAlN coatings was carried out under the following conditions: a TiAl alloy target with an atomic ratio of 40:60 was used, Ar flow rate was constant at 20 sccm, N_2 partial pressure was maintained at 3.2 Pa, target current was kept at 180 A and the substrate bias was set to be - 40 V. The deposition process lasted for 2 h to achieve the expected thickness.

2.2. HCPEB treatment

HCPEB treatment was conducted using a “Hope-I" type HCPEB device. The specific parameters were as follows: background vacuum 5.5 × 10^{-3} Pa, accelerating voltage 27 keV, energy density 5 J / cm^2, pulse duration of 1.5 μs with a pulse interval of 10 s. The diameter of the electron beam was 45 mm to ensure that the coating surface was evenly irradiated, and the pulses number of HCPEB irradiation varied from 5 to 15 pulses.

2.3. Characterization

The phase structure was examined using a Rigaku D/max-2500/pc X-ray diffractometer (XRD) with Cu Kα radiation (λ = 0.154056 nm) operating at 40 kV and 200 mA. The 2θ scanning range was from 30° to 70° with a scanning speed of 8°/ min. The surface morphology of the TiAlN coatings was examined using a field emission scanning electron microscope (SEM, FEI NovaNano 450) equipped with an energy dispersive spectrometer (EDS). The surface roughness was measured using an OLYMPUS OLS4100 type three-dimensional laser scanning microscope (3D-LSM).

Hardness (H) and elastic modulus (E) of the TiAlN coatings before and after HCPEB treatment were determined using a nanoindenter (Anton Paar TTX-NHT3). To eliminate the influence from substrate, a maximum load of 15 mN was adopted to ensure that the maximum penetration depth was always below 10% of the coating thickness. The load function consisted a 30-s loading to the maximum load, followed by a 10-s holding, and then a 30-s unloading. At least 10 points were measured for each sample. The scratch adhesion and wear performance of both the as-deposited and HCPEB treated TiAlN coatings were performed using a multi-functional material property tester (MFT-4000, Lanzhou Huahui Instrument). In scratch test mode, a diamond Rockwell-C stylus (radius 200 μm) was used, and a progressive load increasing from 0 to 150 N at a rate of 100 N/min was applied on the stylus, and the length of the scratch track was 5 mm. Wear tests were performed with the MFT-4000 operating in reciprocating mode at ambient atmosphere. An Al_2O_3 ball with a diameter of 4 mm was used as the counter body. The applied normal load was 10 N, and the stroke length was 5 mm. The linear sliding velocity was set to be 4 mm/s, and the total test time was last for 30 min. The cross-sectional area of wear tracks were characterized by 3D-LSM, and the wear rate (W) can be calculated by:

$$W = \Delta V/(L \cdot F)$$

where F is the applied normal load (N), L is the sliding distance (m), and ΔV is the wear volume (mm^3), which can be obtained by:

$$\Delta V = S_v \cdot L_s$$

where S_v and L_s are the cross-sectional worn area and stroke length, respectively.

3. Results

3.1. Surface morphology

Fig. 1 shows the surface morphology of the as-deposited TiAlN coating and HCPEB treated TiAlN coatings subjected to different pulses of irradiation. Droplets and pinholes can be observed on the as-deposited TiAlN coating surface, as shown in Fig. 1a. The enlarged SEM image (Fig. 1b) shows that the size of spherical droplets can reach up to ~0.8 μm. Fig. 1c and d show the surface morphology of the TiAlN coating underwent 5 pulses of HCPEB irradiation. It is clear that after 5 pulses of irradiation significant surface melting has occurred and the surface status of the TiAlN coating appears even worse. There are many irregular caverns present on the coating surface, which contribute to form a complicated network structure. The inner surface of the cavern wall is covered by numerous spherical particles with an average diameter of ~100 nm, as shown in Fig. 1d. The surface morphology of the TiAlN coating after 10 pulses of HCPEB irradiation is shown in Fig. 1e and f. Craters and microcracks can be readily found on the coating surface, and the diameter of the craters can reach up to ~4 μm. In addition, it seems that the microcracks are originated from these craters and extend laterally. Except for the presence of craters and microcracks, the specimen surface is fairly smooth. It is interesting to note that the coarse droplets shown in Fig. 1a and b are eliminated completely. With a further increase of irradiation pulse to 15 times, as shown in Fig. 1g and h, the surface status of the TiAlN coating improves to a great extent because of the vanishing of the majority of microcracks and craters. Moreover, the enlarged SEM images of Fig. 1f and h reveal that more finer grains (regions noted by the arrows) on the irradiated surface can be obtained after 10 and 15 pulses of HCPEB irradiation.

Fig. 2 shows the 3D morphology images of the TiAlN coatings subjected to different pulses of HCPEB treatment. The presence of local particles and craters on the original coating surface (Fig. 2 a) renders a surface roughness (Ra) of 0.275 μm. After 5 pulses of HCPEB irradiation, however, the surface morphology deteriorates and an increased Ra is determined (as shown in Fig. 2b) due to the formation of the complex network structure on the coating surface. With a further increase in pulse numbers, the surface morphology of the TiAlN coating gradually improves and a minimum Ra value of 0.266 μm is obtained after 15 pulses of irradiation (Fig. 2d).

3.2. Cross-section morphology

Fig. 3 shows the cross-sectional backscattered electron images of the TiAlN coatings before and after HCPEB irradiation. As can be seen from Fig. 3a, the interface between the compact original TiAlN coating and the substrate was sharp, and the thickness was evaluated to be ~2.6 μm. After HCPEB irradiation, as shown in Fig. 3b-d, the interface between the irradiated coating and the substrate became blurred, forming a transition zone of 2–3 μm in thickness. It is believed that the high temperature gradient induced by HCPEB irradiation promoted elemental diffusion between the coating and substrate, resulting in the formation of the transition zone. In addition, a gradual decrease in coating thickness was also observed. The thinning of the TiAlN coatings might result from vaporization of the coating material caused by HCPEB [19]. A closer inspection of Fig. 3b, there were many pores present in the 5-pulse irradiated TiAlN coating. However, the porosity in the TiAlN coatings decreased with increasing pulse numbers, and the structure of

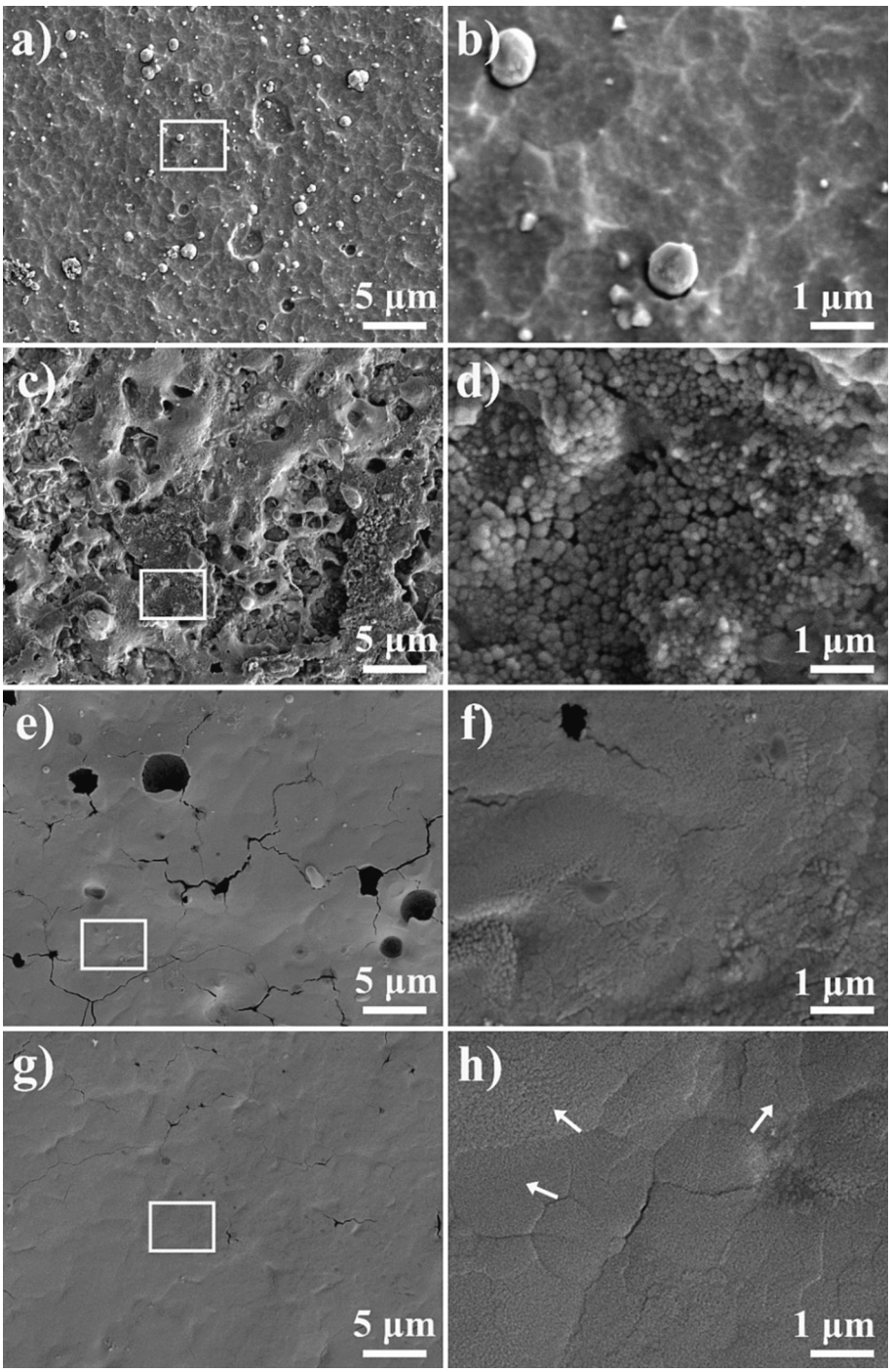

Fig. 1. Typical plan-view SEM images of the original TiAlN coating (a) and HCPEB treated TiAlN coatings subjected to different pulses of irradiation. (c) 5 pulses, (e) 10 pulses, (g) 15 pulses. Higher magnification SEM images for the white rectangle marked area in (a), (c), (e) and (g) are present in (b), (d), (f) and (h), respectively.

the 15-pulsed coating was relatively dense.

3.3. XRD analysis

Fig. 4 shows the XRD diffractograms of both the original and HCPEB treated TiAlN coatings. It can be seen that the spectra for the TiAlN coatings with or without HCPEB irradiation were very similar. The diffraction peaks from the WC-Co cemented carbide substrates can be clearly identified with reference to ICDD 00–051-0939. Additionally, the diffraction peaks centered at 36.6°, 43.5° and 61.7° correspond to the (111), (200) and (220) planes of fcc TiAlN with reference to ICDD 00–038-1420, respectively. It was noticed that the intensity of the TiAlN (111) and (200) peaks intensified with an increase of the irradiation pulse numbers, which might indicate an improved crystallinity of the TiAlN phase. Furthermore, the peak position of TiAlN (111) and (200) planes changed with varying irradiation pulses. The TiAlN (111) diffraction peaks slightly shift to a lower angle except for the coating subjected to 15 pulses of irradiation. While the peak position of the TiAlN (200) plane remained the same except the coating subjected to 5 pulses of irradiation, which shifted to a lower angle. Besides, the peak shifting could also be found for the diffraction peaks from the WC-Co substrate, especially, the peak centered at 48.3°. The diffraction peak

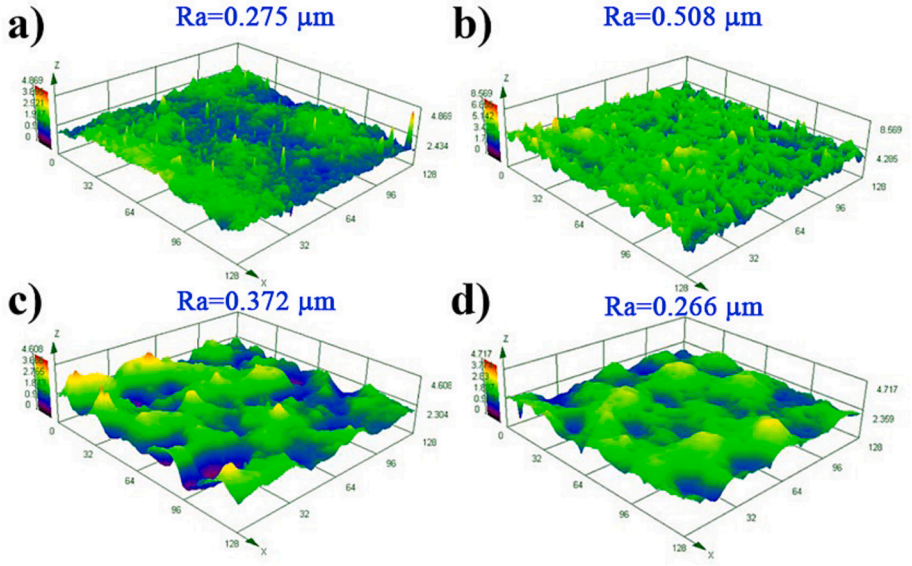

Fig. 2. 3D morphology images of the TiAlN coatings subjected to different pulses of HCPEB treatment: a) original, b) 5 pulses, c) 10 pulses and d) 15 pulses.

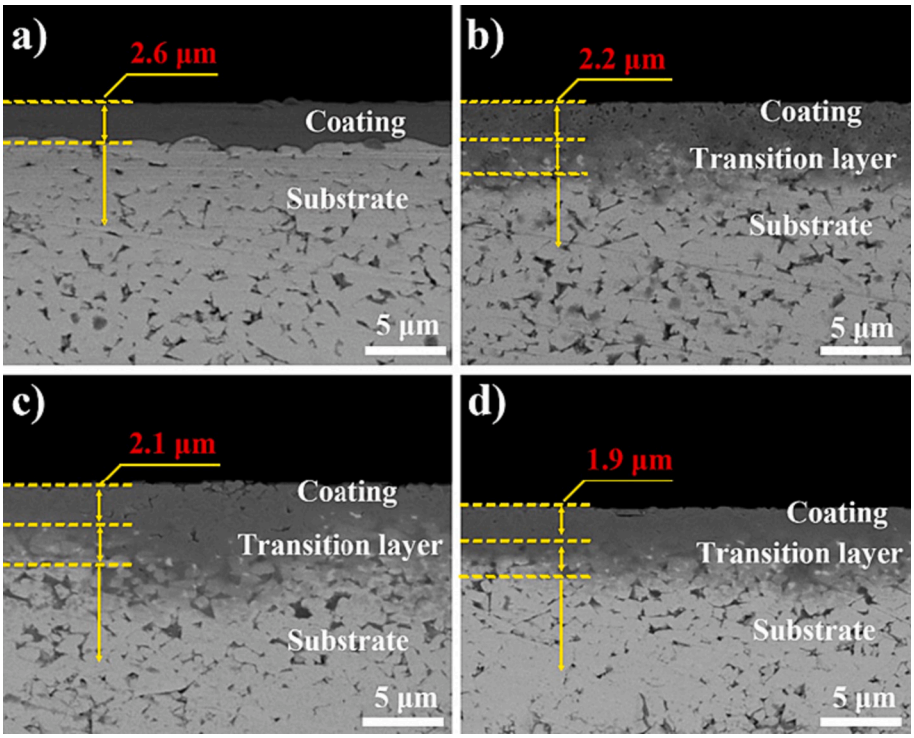

Fig. 3. The cross-section backscattered electron images of the TiAlN coatings before and after HCPEB irradiation: (a) Original, (b) 5 pulses, (c) 10 pulses, (d) 15 pulses.

shifting for both the TiAlN coating and substrate might imply a dramatic change of the residual stress status in the coating after HCPEB treatment [20].

3.4. Mechanical and tribological properties

Fig. 5 shows the nanoindentation load-displacement curve for both the as-deposited and HCPEB irradiated TiAlN coatings. It is clear that the indentation depths for both the original TiAlN coating and HCPEB irradiated TiAlN coatings were always less than 1/10 of the total coating thickness. The hardness (H), elastic modulus (E) of the TiAlN coatings under varying irradiation conditions are present in Fig. 6a. The hardness and elastic modulus of the original TiAlN coating are 24.8 and 357.8 GPa, respectively. Clearly, both the values of H and E increase monotonically with increasing HCPEB pulse number. The maximum values for both H and E are obtained for the TiAlN coating after 15 pulses of HCPEB treatment, reaching up to 33. 4 and 394.5 GPa, respectively. H/E and H^3/E^2 ratios are important indicators for evaluating elastic strain failure and plastic deformation resistance of materials, respectively [21]. It can be seen from Fig. 6b that the changing trends of the H/E and H^3/E^2 ratios of TiAlN coatings are almost identical. With an increase of pulse number, the values of both H/E and H^3/E^2 increase notably, reaching a maximum

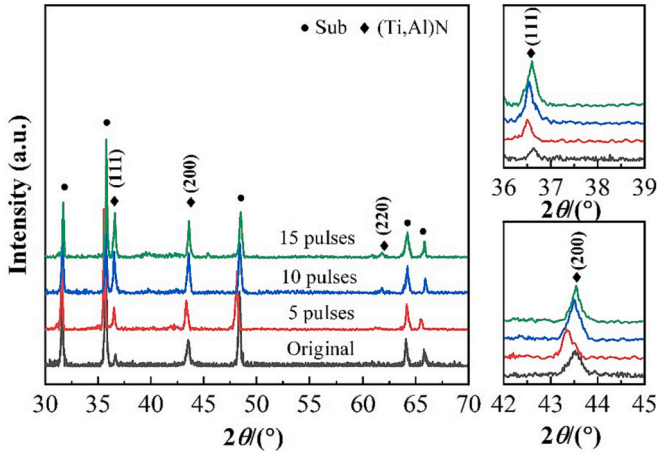

Fig. 4. XRD diffractograms of TiAlN coatings before and after HCPEB irradiation.

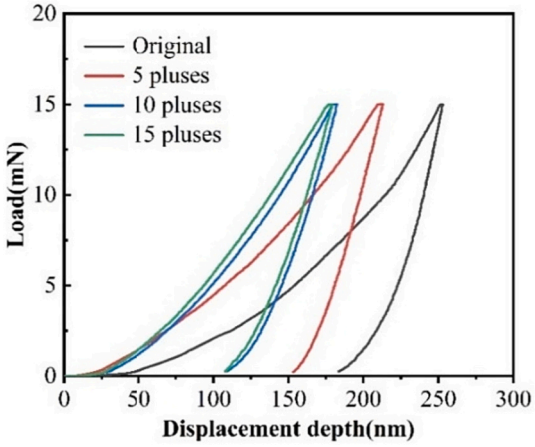

Fig. 5. Nanoindentation load-displacement curve of TiAlN coatings before and after HCPEB irradiation.

for the TiAlN coating treated with 15 pulses of irradiation.

Fig. 7 shows the optical images of the scratch tracks and their corresponding acoustic emission (AE) for both the as-deposited and HCPEB treated TiAlN coatings. In general, two critical loads, Lc_1 and Lc_2, in progressive scratch test are usually defined as the load where the first symptom of cohesive failure (cracking) and the beginning of adhesive failure (buckling, chipping, spalling, etc.), respectively [22,23]. The critical loads Lc_1 are difficult to identify, and the critical loads Lc_2 of the original and irradiated TiAlN coatings are determined by acoustic emission and microscopic observation data. In accordance with Fig. 7, the Lc_2 value for the original TiAlN coating is 64 N. A general increase trend of the Lc_2 value is observed for the TiAlN coatings treated with increasing pulse numbers, and the highest Lc_2 value of 112 N is obtained for the TiAlN coating subjected to 15 pulses of HCPEB irradiation. This indicates that the adhesion strength of TiAlN coatings could be effectively improved by HCPEB treatment.

The friction curves of TiAlN coatings before and after HCPEB irradiation as a function of sliding time are shown in Fig. 8. It can be seen that both the original and HCPEB treated TiAlN coatings have a relatively low friction coefficient of ~0.2 in the initial stage of sliding. For the untreated TiAlN coating, the friction coefficient reach ~0.6 immediately after a short running-in stage, and then decrease rapidly to ~0.5, followed by a gradual increase to ~0.7 till the end of the test. Meanwhile, it takes a longer time (~ 7 min) for the TiAlN coating subjected to 5 pulses of irradiation to complete the running-in stage. The friction coefficient arrives at ~0.5 from 0.2 steadily and increases marginally afterwards. For TiAlN coatings underwent 10 and 15 pulses of irradiation, their friction coefficient stabilized after a short running-in stage (less than 2 min), and the lowest average friction coefficient of ~0.37 is found for the coating treated with 15 pulses of irradiation.

The surface morphology of wear tracks for TiAlN coatings before and after HCPEB irradiation are shown in Fig. 9. Apparent wear tracks can be seen on the surfaces of both the original and TiAlN coatings with 5 pulses of irradiation, while the wear tracks on the TiAlN coatings with 10 and 15 pulses of irradiation become almost indistinguishable, indicating that the wear resistance have been greatly improved. The original TiAlN coating has the maximum wear track width, with a value of 435.55 μm. With an increase of irradiation pulses, the wear track width decreases and reaches the minimum after 15 pulses of irradiation, which is 303.61 μm.

Fig. 10 shows the 2D profile of wear tracks for the TiAlN coatings before and after HCPEB irradiation and their corresponding wear rates. It can be found that the depth of wear track on the original TiAlN coating is ~2.1 μm, which is the deepest among all the coatings. As expected, the original TiAlN coating has the maximum wear rate, with a value of $\sim 5.96 \times 10^{-6}$ mm^3/Nm. In comparison, the maximum wear depth for the 5-pulsed, 10-pulsed, and 15-pulsed TiAlN coatings are 1.9 μm, 1.5 μm and 1 μm, respectively. The wear rates of TiAlN coatings irradiated by 5 pulses and 10 pulses are $\sim 5.4 \times 10^{-6}$ mm^3/Nm and 4.3×10^{-6} mm^3/Nm, respectively. And the lowest wear rate, $\sim 3.3 \times 10^{-6}$ mm^3/Nm, is found for the TiAlN coating subjected to 15 pulses of irradiation, reduced by ~45% compared to that of the original TiAlN coating.

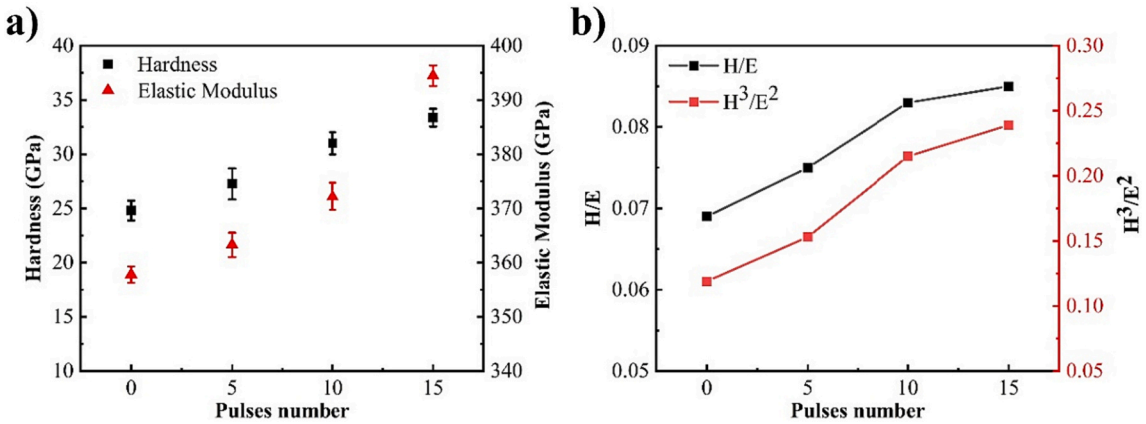

Fig. 6. Mechanical properties of TiAlN coatings as a function of pulses number: (a) hardness and elastic modulus, (b) H/E and H^3/E.[2]

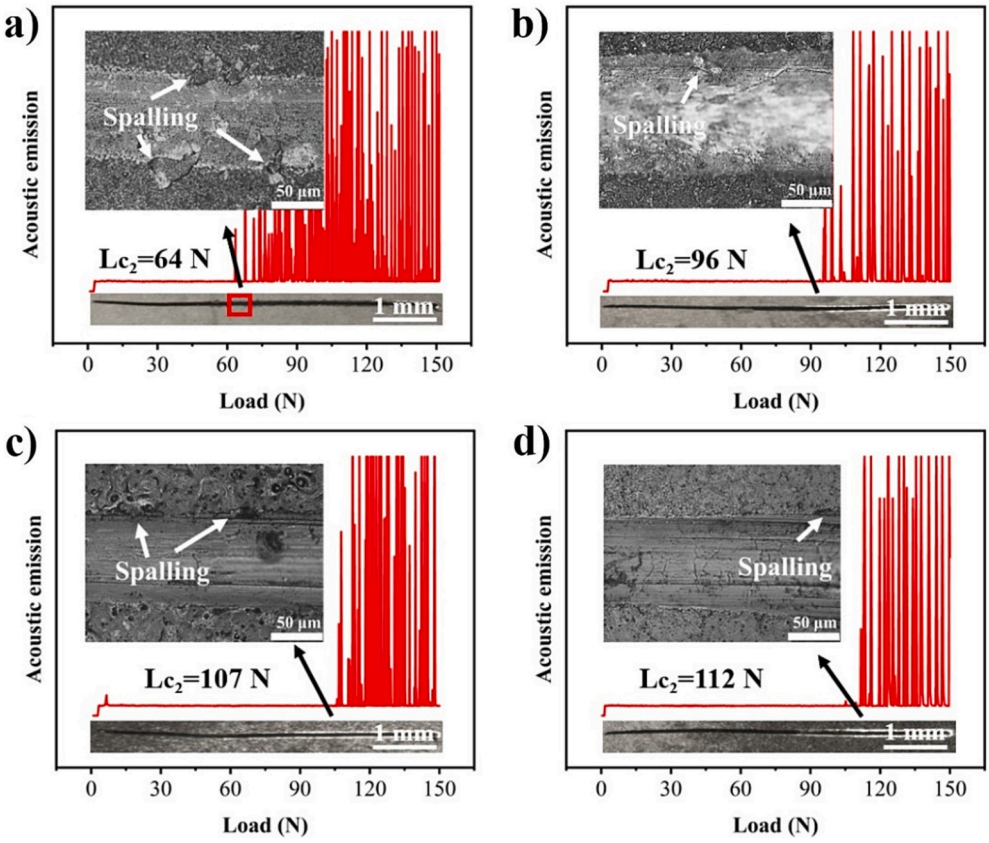

Fig. 7. Optical images of the scratch tracks and corresponding acoustic emission (AE) signal for the original and HCPEB treated TiAlN coatings: (a) Original, (b) 5 pulses, (c) 10 pulses, (d) 15 pulses.

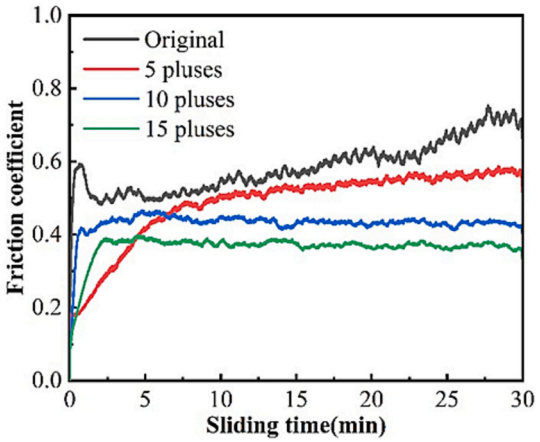

Fig. 8. The friction coefficient of both the original and HCPEB treated TiAlN coatings.

4. Discussion

4.1. Microstructural evolutions introduced by HCPEB irradiation

By comparing the surface morphologies of the as-deposited TiAlN coating with that of the coatings treated by different pulses of HCPEB irradiation (as shown in Fig. 1), it is obvious that the HCPEB pulse number has a considerable influence on the surface morphology and microstructure of the TiAlN coatings. Based on both theoretical and experimental researches, it has been suggested that the formation of craters by pulsed electron beams is the consequence of subsurface melting, followed by the eruption of the subsurface liquid pools due to volume expansion [24,25]. It has been well established that the existence of impurities helps retain locally the heat flux, and consequently serve as nucleation sites for the formation of subsurface melt pools, thus modifying the distribution of crater eruptions [26]. For the arc evaporated TiAlN coatings investigated in this study, these impurities could be grain boundaries and growth defects, i.e. voids or pores. These impurities help form subsurface pools and serve as crater eruption sites, resulting in a large amount of material eruption during the first several pulses of irradiation, leading to an extremely rough surface as shown in Fig. 1c. However, with an increase in pulse numbers, the impurities are gradually removed and crater eruption becomes less significant, and the liquid can flow laterally to supply the lost part due to the crater eruption event. In the meantime, the increase in the melted layer thickness could be regarded as an effective way to protect the material against crater formation, since the interaction of the beam is actually done with the liquid. Accordingly, a significant amount of heat is transferred to the underlying solid by convection at the liquid-solid interface and the formation of craters is difficult to happen [27]. Clearly, when the pulse numbers were increased to 10 or 15 times, the surface morphologies of the TiAlN coatings are greatly improved, especially for the 15 pulses irradiated coating, as shown in Fig. 1g and h.

In addition, an obvious grain refinement effect was found, especially for the TiAlN coatings after 10 and 15 pulses of irradiation. The reason for grain refinement is that during HCPEB irradiation, a high energy is instantly injected onto a very thin layer (less than tens microseconds), causing super-fast heating, melting even evaporation, followed by a rapid solidification and cooling of the surface [28,29]. There will be a large number of nuclei formed in the remelting layer. However, the nuclei do not have time to grow up due to the ultra-fast cooling rate. The ultra-rapid thermo-cycles lead to grain refinement due to the combined

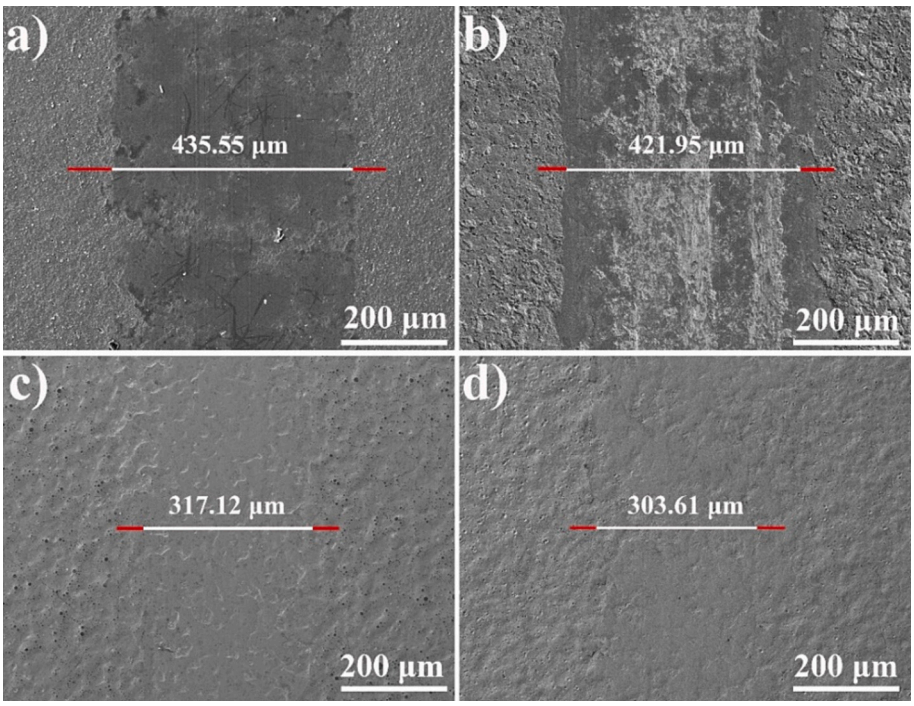

Fig. 9. The wear tracks of TiAlN coatings before and after HCPEB irradiation: (a) Original, (b) 5 pulses, (c) 10 pulses, (d) 15 pulses.

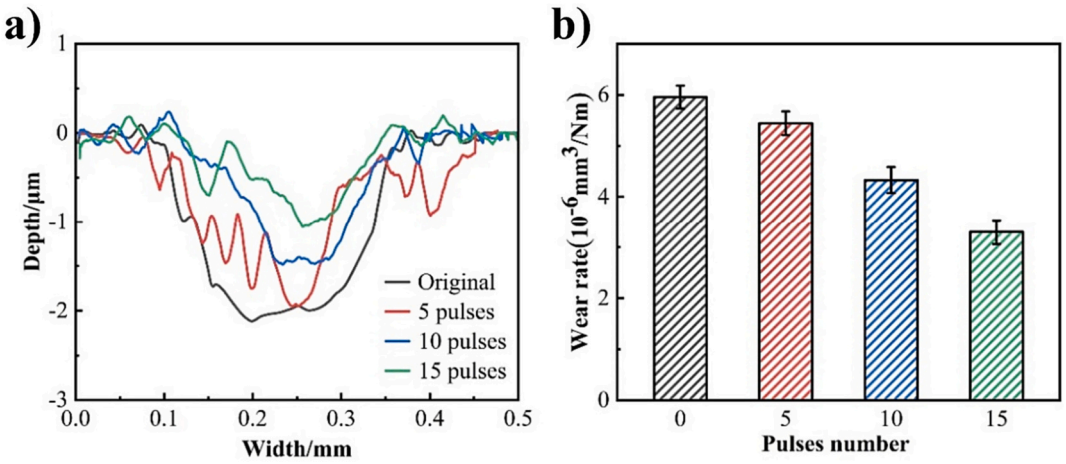

Fig. 10. The wear behavior of both the original and HCPEB treated TiAlN coatings: (a) 2D profiles of wear tracks, (b) wear rate.

effects of increased nucleation rate and reduced grain growth rate, resulting in the formation of ultrafine grains or nanocrystalline structure on the surface [29].

Considering the superfast heating and rapid cooling processes of the HCPEB treatment, high values of internal stresses can be generated. The micro-cracks, which is more evident in Fig. 1e and f, suggested a considerable high value of tensile stress developed after irradiation. Since the microcracks seem to be originated from the craters, these craters are likely to serve as the stress concentration center. The shifting of the XRD peaks, as shown in Fig. 4, also confirmed the presence of residual stress in the HCPEB treated TiAlN coatings.

4.2. Mechanism of the improving mechanical and tribological properties

In terms of the mechanical properties of TiAlN coatings, it is clear that a gradual increase of the values in both H and E was obtained after HCPEB irradiation, as shown in Fig. 6a. The improvement of surface hardness of TiAlN coatings can be considered from the following two aspects. On the one hand, ultrafine nanocrystalline structures were formed on the irradiated coating surface, which contributes to the increase of its hardness according to the Hall-Petch formula ($\sigma = \sigma_0 + kd^{-1/2}$, where σ is the yield strength; K is constant; d is the grain size) [30]. On the other hand, solid solution hardening might come into effect for these HCPEB treated TiAlN coatings. It has been suggested that HCPEB irradiation can change the solid solubility of materials and intensify the diffusion of elements. It has been reported that HCPEB treatment is effective in promoting elemental interdiffusion at interfaces. As a result, the W and Co elements in the cemented carbide substrate could diffuse into the TiAlN coating [31], resulting in hardness improvement of the HCPEB treated TiAlN coatings.

The scratch and wear performance of hard coatings is closely related with their mechanical properties [21]. Coatings with high values of both H/E and H^3/E^2 generally possess strong scratch toughness and wear resistance [23]. In addition, the formation of the transition layer may

contribute to the integrity of the coating system without detachment. The transition layer can minimize the interfacial stress discontinuities and allow the substrate to deform in line with the coating without causing coating cracking or detachment. In accordance with Fig. 6 and Fig. 7, the value of critical load (Lc_2) was in line with the values of both H/E and H^3/E,[2] and the highest critical load was observed for the TiAlN coating treated with 15 pulses of irradiation.

The results of the wear test (Fig. 9 and Fig. 10) show that the major wear mechanism of these TiAlN coatings is abrasive wear. It has been suggested that the wear rate could be influenced by both external and internal factors [32]. Since the wear test conditions are identical, the effect of external factors on the wear rate of these TiAlN coatings are marginal. The internal factors including surface roughness, hardness, H/E and H^3/E^2 ratios on the wear rate of these TiAlN coatings should be considered. G. Ghosh et al. [33] compared the specific wear rate of the as-sprayed and finished WC-Co coatings, and found that the smoothest surface possessed the lowest wear rate. They suggested that the high wear rate for the coatings with rough surface was due to the aggressive three-body abrasion action during wear testing, and they attributed the low wear rate for coating with smooth surface to two-body abrasion. Y. X. Ou et al. [34] studied the wear resistance of CrN/TiN superlattice coatings and found improved wear resistance for the coating with high H, H/E and H^3/E^2 ratios. According to Fig. 1 and Fig. 6, the TiAlN coating subjected to 15 pulses of HCPEB treatment presented the smoothest surface and demonstrated the highest hardness. Thereafter, the lowest wear rate observed in the 15-pulses treated TiAlN coating could be attributed to its low surface roughness, high hardness, H/E and H^3/E^2 ratios.

5. Conclusions

In this work, the arc-ion plated TiAlN coatings were irradiated by HCPEB with different pulses, and the corresponding microstructural, mechanical and tribological properties of these coatings were examined. It was found that the rough droplets on the as-deposited TiAlN coatings were eliminated after HCPEB treatment, resulting in smooth coating surface and reduced grain size. A transition zone was found in the irradiated TiAlN coating, and the thickness of the irradiated coating decreased. No new phase was identified in the irradiated TiAlN coatings. The higher hardness of the HCPEB-treated TiAlN coatings results from grain refinement and solid solution hardening. The high hardness, H/E and H^3/E^2 ratios, and the smoothing of coating surface are the responsible for the improvement of wear resistance of the irradiated TiAlN coatings. Therefore, it is reliable for improving the mechanical and tribological properties of PVD-TiAlN coatings or even all hard nitride coatings by selecting appropriate HCPEB irradiation process.

Credit author statement

Qingfeng Guan: Conceptualization, Funding acquisition, Supervision. **Jing Han**: Investigation, Writing and Editing. **Shiyu Zhou**: Resources. **Jintong Guan**: Review, Resources. **Conglin Zhang**: Review, Resources. **Fuyang Cao**: Conceptualization, Formal analysis, Writing-review & editing. **Xiangming Chen**: Resources.

Declaration of Competing Interest

The authors declare the following financial interests/personal relationships which may be considered as potential competing interests:

Fuyang Cao reports financial support was provided by Hubei Longzhong Laboratory. Conglin Zhang reports financial support was provided by National Natural Science Foundation of China. Jintong Guan reports financial support was provided by Jiangsu Province Natural Science Foundation for Youths. If there are other authors, they declare that they have no known competing financial interests or personal relationships that could have appeared to influence the work reported in this paper.

Data availability

Data will be made available on request.

Acknowledgements

This work was supported by National Natural Science Foundation of China (No. 52001273), Jiangsu Province Natural Science Foundation for Youths (No. BK20201062), and the Open Fund of the Hubei Longzhong Laboratory (Project No.2022KF-11).

References

[1] G. Xian, J. Xiong, H. Zhao, L. Xian, H. Fan, Z. Li, H. Du, Study on the growth and wear behavior of the TiAlN-based composite coating deposited on TiCN-based cermets with different binder phase, Wear 460-461 (2020), 203460.
[2] L. von Fieandt, K. Johansson, T. Larsson, M. Boman, E. Lindahl, On the growth, orientation and hardness of chemical vapor deposited Ti(C,N), Thin Solid Films 645 (2018) 19–26.
[3] Y. Long, J. Zeng, D. Yu, S. Wu, Microstructure of TiAlN and CrAlN coatings and cutting performance of coated silicon nitride inserts in cast iron turning, Ceram. Int. 40 (7, Part A) (2014) 9889–9894.
[4] C. Jarms, H.R. Stock, P. Mayr, Mechanical properties, structure and oxidation behaviour of $Ti_{1-x}Al_xN$-hard coatings deposited by pulsed d.c. plasma-assisted chemical vapour deposition (PACVD), Surf. Coat. Technol. 108–109 (1998) 206–210.
[5] H. Zhao, X.H. Wang, Q.L. Liu, L.J. Chen, Z. Liu, Structure and wear resistance of TiN and TiAlN coatings on AZ91 alloy deposited by multi-arc ion plating, Trans. Nonferrous Metals Soc. China 20 (2010) s679–s682.
[6] M. Egawa, K.I. Miura, M. Yokoi, I. Ishigami, Effects of substrate bias voltage on projection growth in chromium nitride films deposited by arc ion plating, Surf. Coat. Technol. 201 (9) (2007) 4873–4878.
[7] Y. Zhao, G. Lin, J. Xiao, W. Lang, C. Dong, J. Gong, C. Sun, Synthesis of titanium nitride thin films deposited by a new shielded arc ion plating, Appl. Surf. Sci. 257 (13) (2011) 5694–5697.
[8] B. Denkena, B. Breidenstein, L. Gerdes, Residual stress depth distributions in uncoated, PVD coated and decoated carbide cutting tools, in: Proceedings of the 7th International Conference, Coatings in Manufacturing Engineering, 2008.
[9] M.R. Alhafian, J.B. Chemin, Y. Fleming, L. Bourgeois, M. Penoy, R. Useldinger, F. Soldera, F. Mücklich, P. Choquet, Comparison on the structural, mechanical and tribological properties of TiAlN coatings deposited by HiPIMS and cathodic arc evaporation, Surf. Coat. Technol. 423 (2021), 127529.
[10] B. Zhao, X. Zhao, L. Lin, L. Zou, Effect of bias voltage on mechanical properties, milling performance and thermal crack propagation of cathodic arc ion-plated TiAlN coatings, Thin Solid Films 708 (2020), 138116.
[11] K.D. Bouzakis, N. Michailidis, S. Hadjiyiannis, E. Pavlidou, G. Erkens, An effective way to improve the cutting performance of coated tools through annealing, Surf. Coat. Technol. 146-147 (2001) 436–442.
[12] W.J. Liu, J.H. Duan, H.C. Zhao, Y.W. Ye, H. Chen, Effect of cryogenic treatment time on microstructure and tribology performance of TiAlN coating, Surface Topogr. Metrol. Prop. 9 (3) (2021), 035055.
[13] K. Chang, Y. Dong, G. Zheng, X. Jiang, X. Yang, X. Cheng, H. Liu, G. Zhao, Friction and wear properties of TiAlN coated tools with different levels of surface integrity, Ceram. Int. 48 (4) (2022) 4433–4443.
[14] T. Grosdidier, J.X. Zou, B. Bolle, S.Z. Hao, C. Dong, Grain refinement, hardening and metastable phase formation by high current pulsed electron beam (HCPEB) treatment under heating and melting modes, J. Alloys Compd. 504 (2010) S508–S511.
[15] J. Cai, Q. Guan, S. Yang, S. Yang, Z. Wang, Z. Han, Microstructural characterization of modified YSZ thermal barrier coatings by high-current pulsed electron beam, Surf. Coat. Technol. 254 (2014) 187–194.
[16] K.V. Ivanov, M.P. Kalashnikov, Structure and phase composition of "ZrO_2 thin coating – aluminum substrate" system processed through pulsed electron beam irradiation, Appl. Surf. Sci. 534 (2020), 147628.
[17] A.J. Perry, J.N. Matossian, S.J. Bull, D.I. Proskurovsky, P.C. Rice-Evans, T.F. Page, D.E. Geist, J. Taylor, J.J. Vajo, R.E. Doty, V. Rotshtein, A.B. Markov, The effect of rapid thermal processing (RTP) on TiN coatings deposited by PVD and the steel-turning performance of coated cemented carbide, Surf. Coat. Technol. 120-121 (1999) 337–342.
[18] K. Weigel, J. Lu, K. Bewilogua, M. Keunecke, J. Petersen, G. Grumbt, R. Zenker, L. Hultman, Electron irradiation induced modifications of $Ti_{(1-x)}Al_xN$ coatings and related buffer layers on steel substrates, Vacuum 185 (2021), 110028.
[19] J. Cai, Q. Guan, P. Lv, X. Hou, Z. Wang, Z. Han, Surface modification of CoCrAlY coating by high-current pulsed electron beam treatment under the "evaporation" mode, Nucl. Instrum. Methods Phys. Res., Sect. B 337 (2014) 90–96.
[20] J. Cai, L. Ji, S. Yang, X. Wang, Y. Li, X. Hou, Q. Guan, Deformation mechanism and microstructures on polycrystalline aluminum induced by high-current pulsed electron beam, Chin. Sci. Bull. 58 (20) (2013) 2507–2511.

[21] A. Leyland, A. Matthews, On the significance of the H/E ratio in wear control: a nanocomposite coating approach to optimised tribological behaviour, Wear 246 (1) (2000) 1–11.
[22] M. Łępicka, M. Grądzka-Dahlke, D. Pieniak, K. Pasierbiewicz, A. Niewczas, Effect of mechanical properties of substrate and coating on wear performance of TiN- or DLC-coated 316LVM stainless steel, Wear 382 (2017).
[23] F. Cao, P. Munroe, Z. Zhou, Z. Xie, Mechanically robust TiAlSiN coatings prepared by pulsed-DC magnetron sputtering system: scratch response and tribological performance, Thin Solid Films 645 (2018) 222–230.
[24] Y. Qin, J. Zou, C. Dong, X. Wang, A. Wu, Y. Liu, S. Hao, Q. Guan, Temperature–stress fields and related phenomena induced by a high current pulsed electron beam, Nucl. Instrum. Methods Phys. Res., Sect. B 225 (4) (2004) 544–554.
[25] Q. Guan, Q. Zhang, C. Dong, Physical model of stress and deformation microstructures in AISI 304L austenitic stainless steel induced by high-current pulsed Electron beam surface irradiation, ISIJ Int. 48 (2) (2008) 235–239.
[26] K. Zhang, J. Zou, T. Grosdidier, C. Dong, D. Yang, Improved pitting corrosion resistance of AISI 316L stainless steel treated by high current pulsed electron beam, Surf. Coat. Technol. 201 (3) (2006) 1393–1400.
[27] K. Zhang, J. Zou, G. Thierry, C. Dong, Formation and evolution of craters in carbon steels during low-energy high-current pulsed electron-beam treatment, J. Vac. Sci. Technol. A 27 (27) (2009) 1217–1226.
[28] J. Zou, T. Grosdidier, K. Zhang, C. Dong, Mechanisms of nanostructure and metastable phase formations in the surface melted layers of a HCPEB-treated D2 steel, Acta Mater. 54 (20) (2006) 5409–5419.
[29] Q.F. Guan, P.L. Yang, H. Zou, G.T. Zou, Nanocrystalline and amorphous surface structure of 0.45%C steel produced by high current pulsed electron beam, J. Mater. Sci. 41 (2) (2006) 479–483.
[30] C. Zhang, J. Cai, P. Lv, Y. Zhang, H. Xia, Q. Guan, Surface microstructure and properties of Cu-C powder metallurgical alloy induced by high-current pulsed electron beam, J. Alloys Compd. 697 (2017) 96–103.
[31] N. Tian, C. Zhang, P. Lyu, J. Guan, C. Peng, J. Cai, Q. Guan, Impact of high-current pulsed electron beam modification on element diffusion and performance of Ti6Al4V/AISI 316 L stainless steel diffusion bonded joints, Mater. Charact. 204 (2023), 113163.
[32] P. Steinmann, Y. Tardy, H. Hintermann, Adhesion testing by the scratch test method: the influence of intrinsic and extrinsic parameters on the critical load, Thin Solid Films 154 (1) (1987) 333–349.
[33] G. Ghosh, A. Sidpara, P.P. Bandyopadhyay, Understanding the role of surface roughness on the tribological performance and corrosion resistance of WC-Co coating, Surf. Coat. Technol. 378 (2019), 125080.
[34] Y.X. Ou, J. Lin, S. Tong, H.L. Che, W.D. Sproul, M.K. Lei, Wear and corrosion resistance of CrN/TiN superlattice coatings deposited by a combined deep oscillation magnetron sputtering and pulsed dc magnetron sputtering, Appl. Surf. Sci. 351 (2015) 332–343.